ing or exceeding the 0.5 Å precision derived from independent X-ray structures of homologous proteins.[70]

Acknowledgments

This work was supported by a research grant from the Biotechnology Research Development Corporation, and by Southern Illinois University School of Medicine. J.W.S. is a recipient of a National Institutes of Health Research Career Development Award.

[70] J. Janin, *Biochimie* **72,** 705 (1990).

[19] Characterization of Enzyme–Complex Formation by Analysis of Nuclear Magnetic Resonance Line Shapes

By CAROL BETH POST

Introduction

Kinetics and the mechanism of ligand binding can be evaluated from nuclear magnetic resonance (NMR) spectral line shapes of protein–ligand systems.[1,2] It is possible to estimate the rates of dissociation and association or to distinguish between kinetic schemes differing in binding order by an analysis of line widths and peak positions.[3] The range of measurable kinetic rates is determined by the chemical shift differences between the NMR resonances for the two states in exchange since the spectral line shapes are altered when the exchange process occurs on a time scale similar to the inverse of this frequency difference. Rates up to 1000 sec^{-1}, for example, can be evaluated from ^{31}P NMR where chemical shift differences are as large as 3 ppm (i.e., 240 Hz using a 200-MHz spectrometer). The slowest measurable rate is limited by the spectral resolution, usually defined by the resonance line width, and is typically 10 sec^{-1} for ^{31}P NMR of biological systems.

Many published NMR exchange studies involve small molecules where the exchange process being studied is due to a conformational change of the molecule. However, in an enzymatic system the exchange of nuclei between states can occur by the additional processes of ligand binding

[1] D. M. Crothers, P. E. Cole, C. W. Hilbers, and R. G. Shulman, *J. Mol. Biol.* **87,** 63 (1974).
[2] B. D. N. Rao, this series, Vol. 176, p. 279.
[3] H. M. McConnell, *J. Chem. Phys.* **28,** 430 (1958).

or chemical reaction. Thus, a variety of kinetic parameters relevant to enzymatic reactions may be evaluated.[2,4–6]

A general approach involving the analysis of NMR line shapes for obtaining chemical exchange rates is described here. The analysis requires measuring changes in line widths and peak positions as a function of ligand concentration from a simple one-dimensional spectrum. Rate constants are estimated by agreement between the experimental spectra and spectra simulated with a matrix form of the simultaneous Bloch equations for transverse xy magnetization including chemical exchange among all possible sites in a multisite system. This equilibrium method applies to exchange processes with fast or intermediate rates relative to the chemical shift differences. Comparable approaches have been reported for analyzing magnetization transfer NMR data pertaining to exchange processes which are slow on the chemical shift time scale.[5,7–10] In magnetization transfer studies, the change in peak intensities, or longitudinal z magnetization, in response to the selective irradiation of a peak is measured. In other words, a time-dependent intensity change due to a perturbation from equilibrium is analyzed.

The description of the general approach is illustrated with a simple kinetic scheme, followed by the description of a specific example using results from ^{31}P NMR of the enzyme phosphoglucomutase. A cyclic scheme for binding of a substrate analog to the mono- and di-Cd^{2+} complexes of the phospho form of the enzyme is readily characterized with this method. In this system, two magnetic nuclei undergo exchange due to binding, namely, the ^{31}P nucleus of the ligand and that of the phosphoenzyme. Hence, additional constraints are involved; the spectral characteristics of two sets of exchange sites must be consistent with the same association–dissociation rate constants.

Simulation Method

These exchange studies are concerned with transverse magnetization whose description requires complex quantities, as opposed to longitudinal magnetization and real quantities. The matrix form for the exchange system arises from the Bloch equations[11] for the transverse components of

[4] K. V. Vasavada, J. Kaplan, and B. D. N. Rao, *J. Magn. Reson.* **41,** 467 (1980).
[5] C. B. Post, W. J. Ray, Jr., and D. G. Gorenstein, *Biochemistry* **28,** 548 (1989).
[6] W. J. Ray Jr., C. B. Post, Y. Liu, and G. I. Rhyu, *Biochemistry* **32,** 48 (1993).
[7] C. L. Perrin and R. K. Gipe, *J. Am. Chem. Soc.* **106,** 4036 (1984).
[8] M. Grassi, B. E. Mann, B. T. Pickup, and C. M. Spencer, *J. Magn. Reson.* **69,** 92 (1986).
[9] E. R. Johnston, M. J. Dellwo, and J. Hendrix, *J. Magn. Reson.* **66,** 399 (1986).
[10] G. L. Mendz, G. Robinson, and P. W. Kuchel, *J. Am. Chem. Soc.* **108,** 169 (1986).
[11] J. Sandström, *Dynamic NMR Spectroscopy,* Academic Press, London (1982).

magnetization in the rotating frame. (Because spin coupling effects are not a factor in ^{31}P exchange NMR studies, spin coupling is not addressed here.) The time dependences of the transverse components u and v from spin i after the application of a radio frequency pulse B_1 are

$$du/dt = 2\pi v(\nu_i - \nu) - u/T_2^i \tag{1}$$
$$dv/dt = -2\pi u(\nu_i - \nu) - v/T_2^i + \gamma B_1 M_0^i \tag{2}$$

T_2^i is the transverse relaxation time, ν_i is the intrinsic resonant frequency of spin i in the absence of exchange, γ is the gyromagnetic ratio, and M_0^i is the equilibrium z magnetization.

The magnetization in the x–y plane is $M_i = u + iv$, and it has the following time dependence:

$$dM_i/dt = -[1/T_2^i + i2\pi(\nu_i - \nu)]\, M_i + i\gamma B_1 M_0^i \tag{3}$$

The final term in Eq. (3) is a constant factor dependent on experimental conditions which reflects the total equilibrium magnetization intensity of spin i. Equation (3) simplifies to

$$dM_i/dt = -\alpha_i M_i + iC_i \tag{4}$$

with

$$\alpha_i \equiv 1/T_2^i + i2\pi(\nu_i - \nu) \tag{5}$$
$$C_i \equiv \gamma B_1 M_0^i \tag{6}$$

In the case of chemical exchange, Eq. (4) must be modified to account for the interconversion of the nucleus among magnetically inequivalent sites. The kinetic rate constants are defined by

$$\text{Site } i \underset{k_{ji}}{\overset{k_{ij}}{\rightleftharpoons}} \text{Site } j \tag{7}$$

The relative populations may be expressed as

$$f_i/f_j = k_{ji}/k_{ij} \tag{8}$$

and the fractional populations over all possible sites available to that nucleus satisfy the condition

$$\sum_i f_i = 1 \tag{9}$$

The effects of exchange among N sites are accounted for by modifying Eq. (4). The transverse magnetization corresponding to site i in exchange with all other sites j is

$$dM_i/dt = -\alpha_i M_i + if_i C_i - \sum_{j \neq i}^{N} k_{ij} M_i + \sum_{j \neq i}^{N} k_{ji} M_j \tag{10}$$

At equilibrium, $dM_i/dt = 0$ for all spins, and the set of N simultaneous equations in matrix form becomes

$$\mathbf{K} = \mathbf{\Omega}\,\mathbf{G} \tag{11}$$

where the elements of the complex vectors **K** and **G** and the $N \times N$ complex matrix $\mathbf{\Omega}$ are

$$K_i = -if_i C_i \tag{12}$$

$$G_i = M_i \tag{13}$$

$$\Omega_{ii} = -(\alpha_i + \sum_{j \neq i}^{N} k_{ij}) \qquad \Omega_{ij} = k_{ji} \tag{14}$$

The complex spectrum is found by determining **G** as a function of frequency ν, with the absorptive mode being the sum of the N imaginary elements of **G**. The set of simultaneous equations from Eq. (11) was solved with the subroutine LEQT1C in the IMSL library.

Applications

Simple Case

Implementation of the line shape analysis including chemical exchange is illustrated with a simple three-site case:

$$\text{S1} \underset{k_{21}}{\overset{k_{12}}{\rightleftharpoons}} \text{S2} \underset{k_{32}}{\overset{k_{23}}{\rightleftharpoons}} \text{S3} \tag{15}$$

The $\mathbf{\Omega}$ matrix is

$$\mathbf{\Omega} = \begin{bmatrix} -(\alpha_1 + k_{12}) & k_{21} & 0 \\ k_{12} & -(\alpha_2 + k_{21} + k_{23}) & k_{32} \\ 0 & k_{23} & -(\alpha_3 + k_{32}) \end{bmatrix}$$

The simulated spectrum as a function of ν is the summation $M_1^{Im}(\nu) + M_2^{Im}(\nu) + M_3^{Im}(\nu)$.

Rate constants are obtained by finding a set of self-consistent parameters in Ω giving agreement between simulated spectra and measured spectra. The parameters which must be defined are the chemical shift frequency, ν_i, the equilibrium concentration and T_2 for each nuclear spin, and the kinetic rate constants or corresponding equilibrium constant. Titration with one species to give variation in the observed line widths and positions is often necessary for reducing ambiguity in parameter values. Certain parameters, such as equilibrium concentrations or the intrinsic chemical shift frequency, can be readily defined by peak integration and position, respectively, at appropriate points of the titration, or from other NMR spectral data. When an equilibrium constant can be established, it is useful not only for setting ratios of the corresponding rate constants but also for setting concentration values at other points in the titration where peak integration is not possible.

Application to Enzymatic Exchange Systems

To illustrate the application of Eq. (11) to exchange systems involving enzymes and enzyme–ligand complexes, we describe in this section the simulation of the equilibrium spectrum for phosphoglucomutase in the presence of a substrate analog, 1-deoxyglucose 6-phosphate (1-dGlc-6-P).[6] The equilibrium for the complexes formed in the presence of the activating metal ion, Cd^{2+}, is shown in Scheme I, where S_P is 1-dGlc-6-P, $E_P \cdot Cd$ and $E_P \cdot Cd_2$ are the binary and ternary complexes of the phospho form of phosphoglucomutase, and the respective substrate complexes are $E_P \cdot Cd \cdot S_P$ and $E_P \cdot Cd_2 \cdot S_P$. (We use the abbreviation of Cd_x to indicate both mono- and di-Cd^{2+} complexes.) The ^{31}P sites are indexed as indicated by the numbering *Pn* in Scheme I. The number N of sites for Eq. (10), or elements i for Eq. (11), is defined by the number of chemically distinct ^{31}P nuclei. Compared to the linear kinetic scheme discussed above, the relative complexity of this system arises not only from the cyclic nature but also from the fact that there are two distinct ^{31}P nuclei present in each of the enzyme–substrate complexes. It should be noted that the simulation procedure outlined here applies equally well to enzymatic mix-

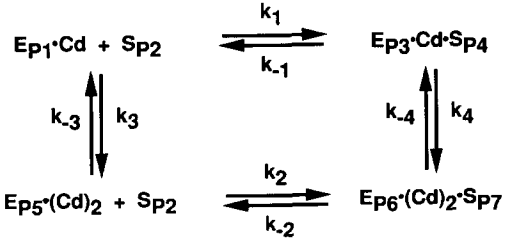

SCHEME I

tures for which bond breaking and bond making are included in the equilibrium.

The rate constants in the elements of $\mathbf{\Omega}$ [Eq. (14)] are the pseudo-first-order rate constants corresponding to the exchange of ^{31}P nuclei. For Scheme I, $\mathbf{\Omega}$ is shown in Eq. (16). Elements of $\mathbf{\Omega}$ equal to 0 correspond

$$\Omega = \begin{bmatrix} -\alpha_1 - k_1[S_{P2}] - k_3 & 0 & k_{-1} & 0 & k_{-3} & 0 & 0 \\ 0 & -\alpha_2 - k_1[E_{P1}(Cd)] - k_2[E_{P5}(Cd)_2] & 0 & k_{-1} & 0 & 0 & k_{-2} \\ k_1[S_{P2}] & 0 & -\alpha_3 - k_{-1} - k_4 & 0 & 0 & k_{-4} & 0 \\ 0 & k_1[E_{P1}(Cd)] & 0 & -\alpha_4 - k_{-1} - k_4 & 0 & 0 & k_{-4} \\ k_3 & 0 & 0 & 0 & -\alpha_5 - k_2[S_{P2}] - k_{-3} & k_{-2} & 0 \\ 0 & 0 & k_4 & 0 & k_2[S_{P2}] & -\alpha_6 - k_{-2} - k_{-4} & 0 \\ 0 & k_2[E_{P5}(Cd)_2] & 0 & k_4 & 0 & 0 & -\alpha_7 - k_{-2} - k_{-4} \end{bmatrix} \tag{16}$$

to nonexistent exchange processes.

Fitting of the simulated spectra to the experimental spectra for the titration of phosphoglucomutase with 1-dGlc-6-P was carried out in an interative fashion. Values for the intrinsic resonance frequencies, ν_i, and T_2^i were obtained from independent NMR spectra ($E_P \cdot Cd_x$, S_P) or limiting points of the titration ($E_P \cdot Cd_x \cdot S_P$). Values for the equilibrium constants for binding S_P to either $E_P \cdot Cd_x$ enzyme form were estimated from the peak areas observed in the presence of 1.28 enzyme equivalents of 1-dGlc-6-P (middle spectrum, Fig. 1). To begin the fitting procedure, the kinetic rates in Scheme I were estimated based on the variation in line widths and peak position over the titration given the chemical shift differences of the nuclei in exchange. Consistency was maintained between the ratios k_1/k_{-1} and k_2/k_{-2} with the respective binding constants for S_P. The kinetic rates for Scheme I were altered in an iterative fashion so as to remove discrepancies between the simulated and measured spectra knowing the changes in line shape that are characteristic of transitions from slow to intermediate to fast exchange conditions. Certain T_2^i and ν_i values were also altered to improve agreement. The final parameter values used in the simulation shown in Fig. 2 are in Table I. Only limiting values can be determined for certain rate constants when the rates are beyond the limits of discrimination defined by the chemical shift differences.

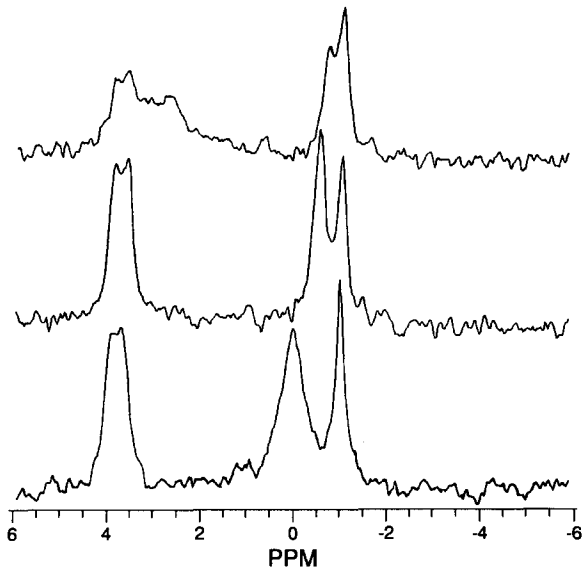

FIG. 1. ^{31}P NMR spectroscopy of the ^{113}Cd complex of the phospho form of phosphoglucomutase in the presence of varying concentrations of 1-deoxyglucose 6-phosphate. The ^{113}Cd complex of the phosphoenzyme, Ep · Cd, was obtained by the addition of 1.5 equivalents of ^{113}Cd-labeled cadmium acetate to a solution of the metal-free phosphoenzyme; the final enzyme concentration was 1.3 m*M*, in 20 m*M* Tris-HCl, pH 7.5, containing 10% D_2O. Spectra were measured with a 4.2-sec recycle time, a 60° pulse angle, and 4096 transients at a 80.1-MHz field for ^{31}P. A line broadening factor of 5 Hz was applied before Fourier transformation. Chemical shifts refer to trimethylphosphate. The doublet splitting at 3.75 ppm is due to ^{113}Cd-^{31}P coupling. Spectra were produced after addition of small volumes containing 0.64 (top), 0.98 (middle), and 1.28 (bottom) equivalents of 1-dGlc-6-P.

The capabilities of this approach include definition of the kinetic rate constants within time limits determined by the nature of the changes in line widths and peak positions, and the chemical shift differences $\Delta\nu = (\nu_i - \nu_j)$ between nuclei in exchange. For the case of 1-dGlc-6-P binding to phosphoglucomutase, an approximate value of $\Delta\nu$ of 200 Hz [i.e., $\nu_i(E_P \cdot Cd_2) - \nu_i(E_P \cdot Cd_2 \cdot S_P)$] defined lower limits for k_3 and k_{-3} of approximately 500 and 1000 sec^{-1}, respectively, whereas a $\Delta\nu$ value around 20 Hz [i.e., $\nu_i(E_P \cdot Cd \cdot S_P) - \nu_i(E_P \cdot Cd_2 \cdot S_P)$] defined upper limits for k_4 and k_{-4} of approximately 16 and 12 sec^{-1}, respectively. (The exchange path determining the lower limit for k_3 and k_{-3} is the enzymatic phosphorus exchange $E_P \cdot Cd_2 \rightleftharpoons E_P \cdot Cd \rightleftharpoons E_P \cdot Cd \cdot S_P$.) A further result of the line shape analysis was differentiating between two possible kinetic schemes. With the spectra in Fig. 1 it was possible to eliminate a linear kinetic

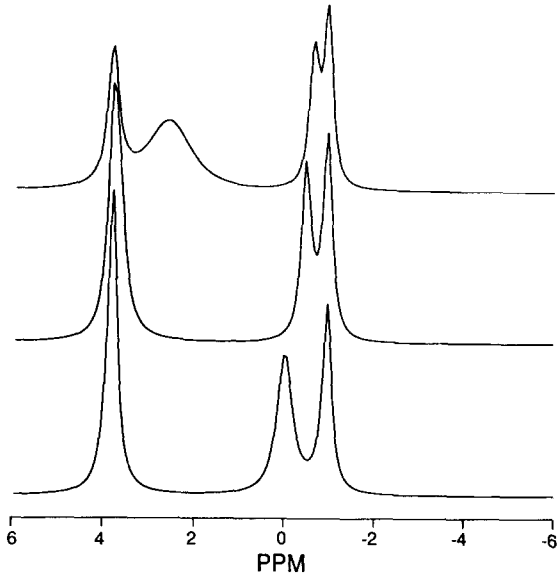

FIG. 2. Line shape simulations of the ^{31}P NMR spectra in Fig. 1. In these simulations the coupling to ^{113}Cd was ignored (see Fig. 1), as were possible intensity differences arising from disparate T_1 values. The ratios of enzyme–Cd^{2+} complex to deoxy sugar used in the simulations are the same as those given in the legend to Fig. 1.

scheme involving two binding modes in which an initial $E_P \cdot Cd \cdot S_P$ complex converts to a second $E_P^* \cdot Cd \cdot S_P$ complex; a linear scheme was not consistent with the spectra even allowing all kinetic constants and ν_i to vary.

TABLE I
PARAMETERS FOR SPECTRAL SIMULATION SHOWN IN FIG. 2[a]

Parameter	P1	P2	P3	P4	P5	P6	P7
δ_i (ppm)[b]	1.60	1.20	3.75	−0.75	1.60	3.75	−1.07
T_2^i	0.021	0.16	0.016	0.021	0.021	0.016	0.021
f_i							
Top	0.145	0.002	0.170	0.172	0.120	0.218	0.218
Middle	0.014	0.026	0.215	0.215	0.007	0.262	0.262
Bottom	0.002	0.121	0.193	0.193	0.001	0.245	0.245
k_1	k_{-1}	k_2	k_{-2}	k_3	k_{-3}	k_4	k_{-4}
307,200	1000	35.2	0.0452	≥500	≥1000	≤16.3	≤12.5

[a] Total enzyme concentration was 1.3 mM, and the top, middle, and bottom spectra were simulated for addition of 0.64, 0.98, and 1.28 equivalents of 1-dGlc-6-P, respectively.
[b] The ^{31}P spectra were measured in a 80.1-MHz field so that $\upsilon_i = 80.1 \times \delta_i$.

Acknowledgment

The author is grateful to William J. Ray, Jr. Much of this work was initiated by collaboration with him.

[20] Computer Simulations of Nuclear Overhauser Effect Spectra of Complex Oligosaccharides

By C. ALLEN BUSH

Introduction

Structures of small proteins in solution can now be solved by nuclear magnetic resonance (NMR) spectroscopy to an accuracy comparable to that previously obtained only by X-ray crystallography. The method involves measurement of the ^{1}H NMR spectrum, assignment of all the ^{1}H NMR signals to individual protons of the protein, and measurement of ^{1}H nuclear Overhauser effects (NOE) which are then interpreted as measures of the distance between protons. These data are incorporated in molecular modeling algorithms to derive the protein structure.[1] Although this method has enjoyed its most spectacular success with protein structures, it has also been applied to nucleic acids, especially to small DNA duxplexes,[2,3] and the general approach is valid for any biopolymer. It has been applied to small peptides and to protein cofactors[4] as well as to oligosaccharides.[5,6] Competing methods for analysis of these NOE data in terms of structure differ in detail with no obvious consensus on methodology. This field is certainly not mature, and it may be that different methods lend themselves well to different biopolymer applications.

Among the methods which have been proposed for the interpretation of NOE-derived distance data in terms of biopolymer structure, the simplest and the one which has been used most commonly in proteins is the "isolated spin pair" approximation which begins with the assumption

[1] R. Powers, D. S. Garrett, C. J. March, E. A. Frieden, A. M. Gronenborn, and G. M. Clore, *Science* **256,** 1673 (1992).
[2] B. R. Reid, *Q. Rev. Biophys.* **20,** 1 (1987).
[3] D. J. Patel, L. Shapiro, and D. Hare, *Q. Rev. Biophys.* **20,** 35 (1987).
[4] K. D. Olsen, H. Won, R. S. Wolfe, D. R. Hare, and M. F. Summers, *J. Am. Chem. Soc.* **112,** 5884 (1990).
[5] L. Poppe, R. Stuikeprill, B. Meyer, and H. vanHalbeek, *J. Biomol. NMR* **2,** 109 (1992).
[6] C. A. Bush, *Curr. Opin. Struct. Biol.* **2,** 655 (1992).